

supporting information

Multifunctional Chitosan-based Porous Membrane for pH-responsive Antimicrobial and Promoting Infected Wound Healing

Shan Pu^a, Jiale Zhang^a, Chaoting Shi^a, Xiandeng Hou^{a,b}, Ka Li^c, Jinhua Feng^{c*}, Lan Wu^{a*}

^a Analytical & Testing Center, Sichuan University, Chengdu 610064, Sichuan, China.

^b Key Laboratory of Green Chemistry & Technology, Ministry of Education, College of Chemistry, Sichuan University, Chengdu 610064, Sichuan, China.

^c West China School of Nursing, Sichuan University/Department of Biliary, West China Hospital, Sichuan University, Chengdu 610064, Sichuan, China.

*Corresponding author: Jinhua Feng (fengjinhua327@163.com), Lan Wu (wulan@scu.edu.cn)

S1. Materials and methods

S1.1. Reagents

Chitosan (CS) was purchased from Aladdin (Shanghai, China), and its physiochemical characterization was given in S1.3. 2-methylimidazole ($C_4H_6N_2$), and glacial acetic acid (CH_3COOH) were purchased from Aladdin (Shanghai, China). Hydroxyapatite (HAp) was developed by the Laboratory of Biomaterials Engineering Research Center, Sichuan University (Chengdu, China). Zinc nitrate ($Zn(NO_3)_2$), sodium hydroxide (NaOH), and polyethylene glycol (PEG, MW: 20,000) were purchased from Kelong Chemical Co., Ltd (Chengdu, China). LB broth was obtained from Qingdao Haibo Biotechnology Co., Ltd (Qingdao, China). *Escherichia coli* (*E. coli*) and *Staphylococcus aureus* (*S. aureus*) were purchased from the Shanghai Center for Preservation Biotechnology (Shanghai, China). Dextrose citrate solution (ACD blood anticoagulant) was purchased from Sangong Bioengineering Co., Ltd (Shanghai, China), and 3-(4,5-dimethylthiazol-2)-2,5-diphenyltetrazolium bromide (MTT) was purchased from Guangzhou Saikoku Bio-technology Co., Ltd (Guangzhou, China). Rat IL-6 ELISA KIT, Rat IL-10 ELISA KIT and Rat TNF- α ELISA KIT were purchased from Shanghai Thrive Color Biotechnology Co., Ltd (Shanghai, China). Mouse fibroblasts (L929) were purchased from Procell (USA).

All reagents used in this work were analytically pure unless otherwise stated.

S1.2. Apparatus

A Nicolet Model 6700 Fourier Transform Infrared Spectrometer (FT-IR Thermo Electron USA) was used to characterize and deduce the chemical structure and functional groups of the materials. The X' Pert Pro MPD type powder X-ray diffractometer (PXRD Philips Netherlands) was used to analyze the physical composition of materials. Model JSM-7500F Scanning Electron Microscope (SEM Japan Electron) was used to analyze the morphology and elemental content of materials. An electronic universal materials testing machine (AG 5985 Instron, USA) was used to determine the mechanical properties of materials. PLUS 384 enzyme marker (Molecular Devices, USA) was used for the determination of absorbance. An

iCAP Q ICP-MS (Thermo Fisher, Germany) was used to measure the release of Zn^{2+} and Ca^{2+} from the prepared membranes.

S1.3. Physiochemical characterizations of the purchased CS

S1.3.1. Molecular weight distributions

The molecular weight distribution of CS was determined by gel permeation chromatography on a waters 2695 high performance liquid chromatograph equipped with a 2410 differential refractive index detector and an Empower workstation. A Ultrahydrogel TMLinear 300*7.8 mmid column was selected. 0.1 M sodium nitrate was used as the mobile phase with a flow rate of 0.5 ml/min and a column temperature of 0.5 ml/min.

S1.3.2. Viscosity

0.5 g of CS was added to 2 % (v/v) acetic acid and stirred at 80 °C for 3 h to dissolve CS completely, followed by testing in a rotational viscometer (NDJ-79, Shanghai, China). Measurements were performed immediately after preparation of homogeneous chitosan dissolution completed. The reported viscosity was the average of three measurements.

S1.3.3 Degree of deacetylation

0.5 g of CS was accurately weighed and put into a 50 mL centrifuge tube. Then, 18 mL HCl (0.3 M) was added and stirred at room temperature for 2 h to completely dissolve the CS. Finally, the above mixed solution was titrated by the sodium hydroxide titration solution (0.15 M) and three drops of methyl orange solution were added as the indicator until it turned to be orange.

The deacetylation degree (DD) of the CS was calculated according to the following formula (1):

$$DD(\%) = \frac{c_1v_1 - c_2v_2 \times 0.016}{G \times (100 - W) \times 9.94\% \times 100\%} \quad (1)$$

DD (%) is the degree of deacetylation. C_1 and C_2 are the molar concentrations of the HCl and NaOH solutions (mol/L), respectively. V_1 and V_2 are the volume of the HCl and NaOH solutions (mL), respectively. G is the initial mass of CSP(g). W is the

weight after dry weight loss of CS (g). 0.016 is the mass of amino groups (g) required for 1 mol/L HCl consuming. 9.94 % is the mass percentage of NH₂ in fully deacetylated CS.

S1.3.4 Elemental analysis

The C, H and N contents of CS were determined using a Vario EL cube elemental analyzer. 2 mg of each sample was collected dry and placed in a tin capsule and heated in a combustion tube at approximately 1800°C. The weight percentage of C, H and N was then determined using a thermal conductivity detector.

S1.4. Performance of physicochemical property

The mechanical strength, porosity and swelling ratio of CH, CHZ-2, CHZ-5, CHZ-10, and CHZ-20 were examined separately to investigate the effect of the loading of ZIF-8 on the physicochemical properties of the membranes.

S1.4.1. Mechanical strength test

Tensile tests were carried out at room temperature to determine the mechanical strength of the membranes ¹. The membranes were cut into rectangles (50 mm long and 10 mm wide) and the stretching ratio was maintained at 10 mm/min.

S1.4.2. Porosity test

The porosity was determined using the specific gravity bottle method ². First, the specific gravity bottle was filled with anhydrous ethanol, and the weight was recorded as W₁. The membrane (mass recorded as W_f) was then immersed in the above specific gravity flask and degassed by ultrasound. Subsequently, the specific gravity bottle was refilled with anhydrous ethanol and the weight recorded as W₂. Finally, the membrane was removed and the weight of the remaining liquid and the hydrometer was recorded as W₃. Porosity (P) was calculated according to equation (2).

$$P = \frac{W_2 - W_3 - W_f}{W_1 - W_3} \times 100\% \quad (2)$$

S1.4.3. Swelling ratio test

The procedure for determining the swelling ratio of the membranes was as follows: a dry membrane of mass m₀ was taken and then placed in deionized water at 37 °C until

the weight no longer increased. The surface of the membrane was gently drained with filter paper and its mass was weighed and recorded as m_w . Finally, the swelling ratio (SR (%)) of the membrane was calculated by equation (3).

$$SR(\%) = \frac{m_w - m_0}{m_0} \times 100\% \quad (3)$$

S1.5. Zn²⁺ and Ca²⁺ release assay

To assess the pH-responsive Zn²⁺ and Ca²⁺ release capacity, the same mass of CH, CHZ-2, CHZ-5, CHZ-10, and CHZ-20 were immersed in PBS buffer at different pH values (5 mL, pH = 7.4 or 5.5). Incubation was continued at 37°C for 14 days and the supernatant was collected at intervals for determination of Zn²⁺ and Ca²⁺ concentration by ICP-MS.

S1.6. Performance of *in vitro* biology

S1.6.1. Hemostatic ability assay

Citrated whole blood was obtained by mixing ACD blood anticoagulant solution with rat blood (1:9 volume ratio). Square (10 mm × 10 mm) gauze (control), CH, CHZ -2, CHZ-5, CHZ-10 and CHZ-20 were placed in centrifuge tubes and incubated at 37°C for 20 min. Then 100 μL of fresh ACD anticoagulant solution was dripped onto the sample surface and 10 μL of 0.02 M CaCl₂ solution was added separately and incubated for 5 min at 37°C on a constant temperature shaker. Next, 30 mL of PBS buffer was slowly added to the centrifuge tubes and centrifuged at 1000 rpm for 1 min. The absorbance of the supernatant at 540 nm was measured using an enzyme marker, and recorded as A_s . The absorbance at 540 nm of a mixture of 100 μL fresh citrated whole blood and 30 mL PBS was used as a reference (A_b). The coagulation index (BCI) was calculated as shown in Equation (4).

$$BCI = \frac{A_s}{A_b} \times 100\% \quad (4)$$

S1.6.2. Hemolysis assay

Square (10 mm × 10 mm) CH, CHZ-2, CHZ-5, CHZ-10 and CHZ-20 were placed in centrifuge tubes with 1 mL of PBS buffer and incubated at 37°C for 10 min. Then 1

mL of diluted blood ($V_{\text{Blood}}/V_{\text{PBS}}=1/10$) was added and the incubation continued for 1 h. After centrifugation at 1000 rpm for 5 min, 200 μL of the supernatant was collected for absorbance at 540 nm. TritonX-100 (0.1%) and PBS buffer were used as positive and negative controls, respectively. The hemolysis ratio was obtained by equation (5).

$$Hemolysis (\%) = \frac{(A_s - A_p)}{(A_t - A_p)} \times 100\% \quad (5)$$

In the formula, A_s , A_p and A_t were the absorbance values at 540 nm for the sample suspension, PBS buffer and 0.1% TritonX-100, respectively.

S1.6.3. Cell cytotoxicity assay

ISO 10993-5:1992 extraction method was used to evaluate the cytotoxicity of the sample membranes^{3, 4}. CHZ-10 (10 \times 10 mm, weighing approximately 10 mg) was immersed in 1 mL of cell culture solution for 24 h. The extracts were subsequently diluted to 20, 50, 100, 200, and 500 $\mu\text{g}/\text{mL}$ with cell culture solution.

L929 cells were used as a model to detect cell proliferation in culture medium by MTT assay. Firstly, L929 cells in logarithmic growth phase were taken to make single cell suspension. The single cell suspension was then inoculated in 96-well plates and incubated at 37°C in 5% CO₂. After the cells were attached to the wall, the control, and the extract groups (20, 50, 100, 200, 500 $\mu\text{g}/\text{mL}$) were set up with four parallel samples in each group. After 1 d, 2 d and 3 d of interaction of the material with the cells, the supernatant was discarded and 200 μL of 0.5 mg/mL MTT solution was added to each well. The plates were gently shaken several times, and incubation was continued at 37°C in 5% CO₂ for 4 h. The supernatant was discarded again and 150 μL dimethyl sulfoxide (DMSO) was added to each well. The absorbance of each well was measured at 570 nm after shaking at low speed for 10 min to completely dissolve the crystals.

S1.6.4. Cell migration assay

L929 cells were used for the migration assay. A cell suspension was first prepared and diluted to 1×10^5 CFU/mL. Cell suspensions of the above concentrations were inoculated into 24-well plates, 1 mL per well, in four groups of three parallel samples each. The cells were cultured at 37°C in 5% CO₂ for 24 hours to allow the cells to

attach to the wall. Crosses were made on the well plates containing the cells and the medium was replaced with the experimental group. Basic media, basic media containing 30 $\mu\text{g/L}$ Zn^{2+} , 4 $\mu\text{g/L}$ Ca^{2+} and CHZ-10 extracts were used as the control and experimental groups, respectively. Finally, the cells continued to be placed in the incubator and photographed at 0 h and 9 h to observe cell migration.

S1.6.5. Anti-inflammatory indicators assay

The supernatant of CHZ-10 was collected for ELISA assay when RAW264.7 was inoculated in the various immersion fluids and cultured for 3 days. The mouse TNF- α , IL-6, and IL-10 ELISA kits were used to measure the secretion of TNF- α , IL-6 and IL-10.

S1.6.6. Angiogenesis indicators assay

The supernatant of CHZ-10 was collected for immunofluorescence assay when HUVECs was inoculated in the various immersion fluids and cultured for 3 days. The CD31 and VEGF were colored green and red fluorescent, respectively. Image J was further used to count the average intensity of fluorescence of the pictures.

S2. Results and discussion

S2.1. Characterization of physicochemical properties of CHZ membranes

Table S1. Physicochemical properties of the purchased CS.

Mw (kDa)	Viscosity (mpa.s)	DD (%)	H (wt%)	N (wt%)	C (wt%)
874.35	44.5	97.70%	7.21	7.67	41.20

Mw was the weight-average molecular weight, DD was the deacetylation degree of CS.

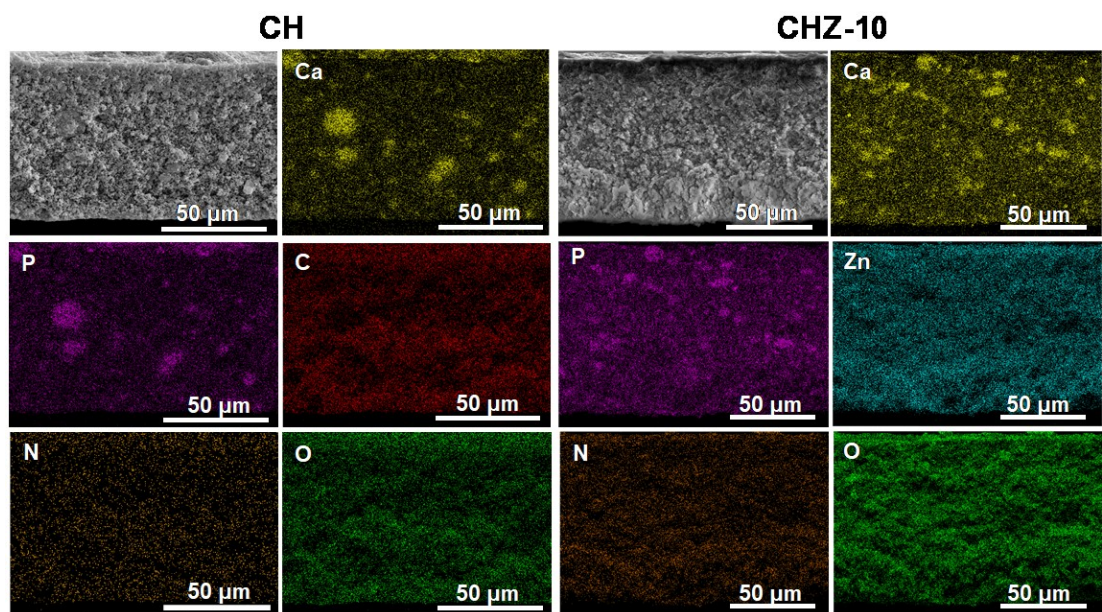


Fig. S1 Mapping of CH and CHZ-10 membranes. The CH membrane contained the elements of Ca, P, C, N and O, while the CHZ-10 membrane contained the element of Zn evenly distributed in addition Ca, P, C, N and O. ZIF-8 was successfully attached to the CH membrane by in situ growth.

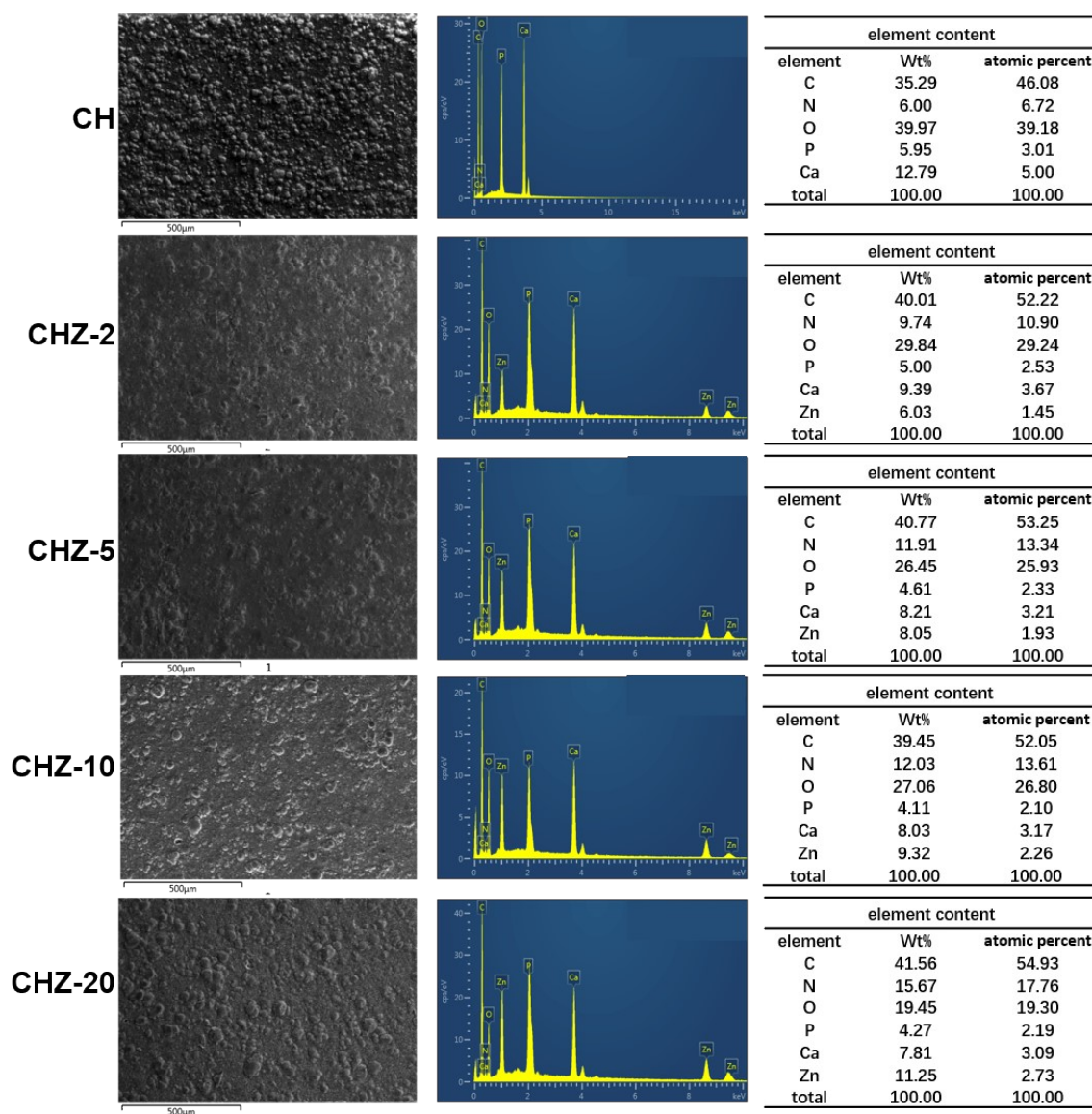


Fig. S2 EDS results of CH and CHZ membranes. It could be seen that as the concentration of Zn^{2+} used in the synthesis process increases, the final Wt% of Zn element on the membrane was higher, indicating the successful synthesis of CHZ membranes with a concentration gradient of ZIF-8 loading.

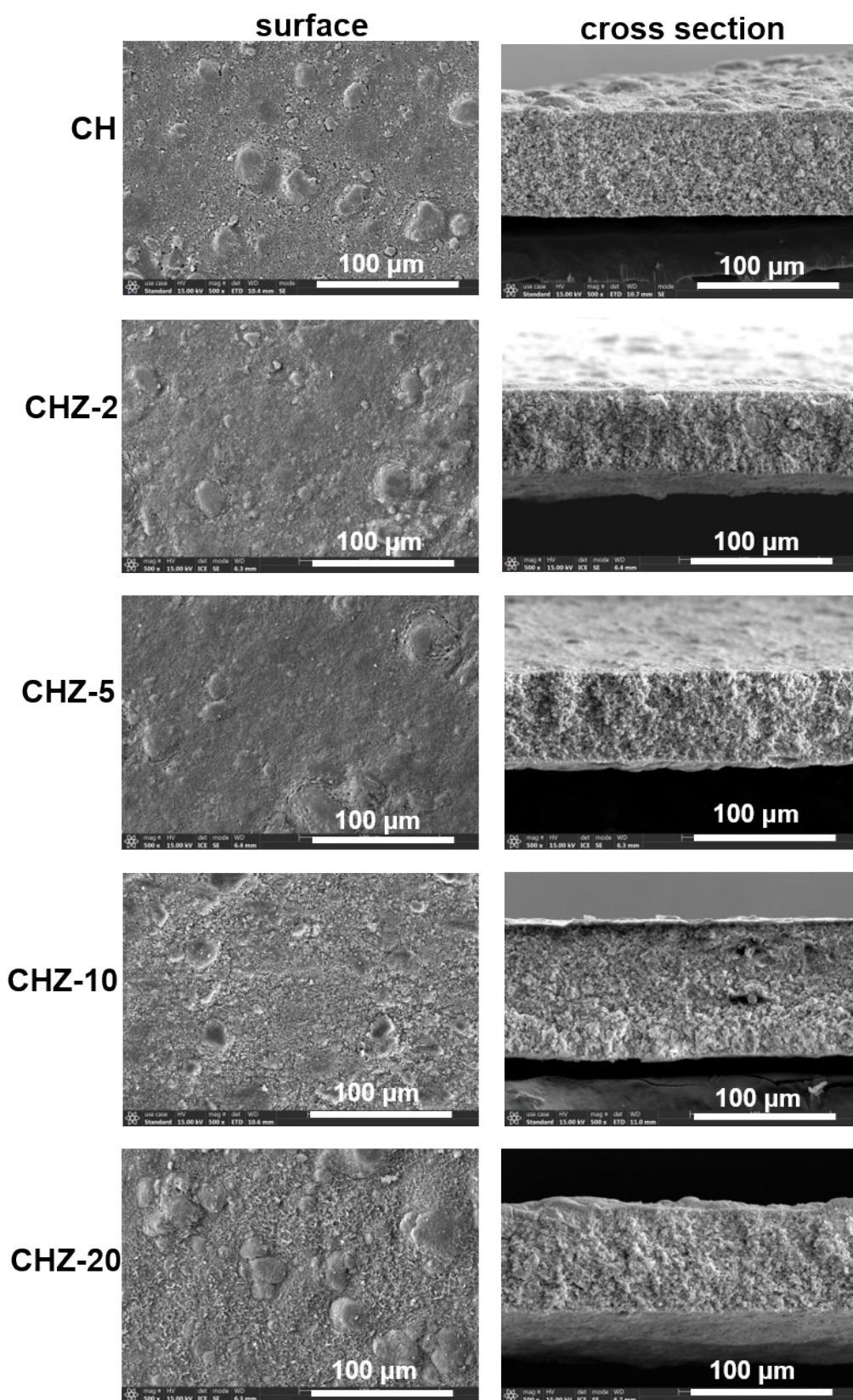


Fig. S3 Surface and cross-section SEM images of CH and CHZ membranes at low magnification. At low magnification, the morphology of the surface and cross-section remained almost unchanged even with different loadings of ZIF-8.

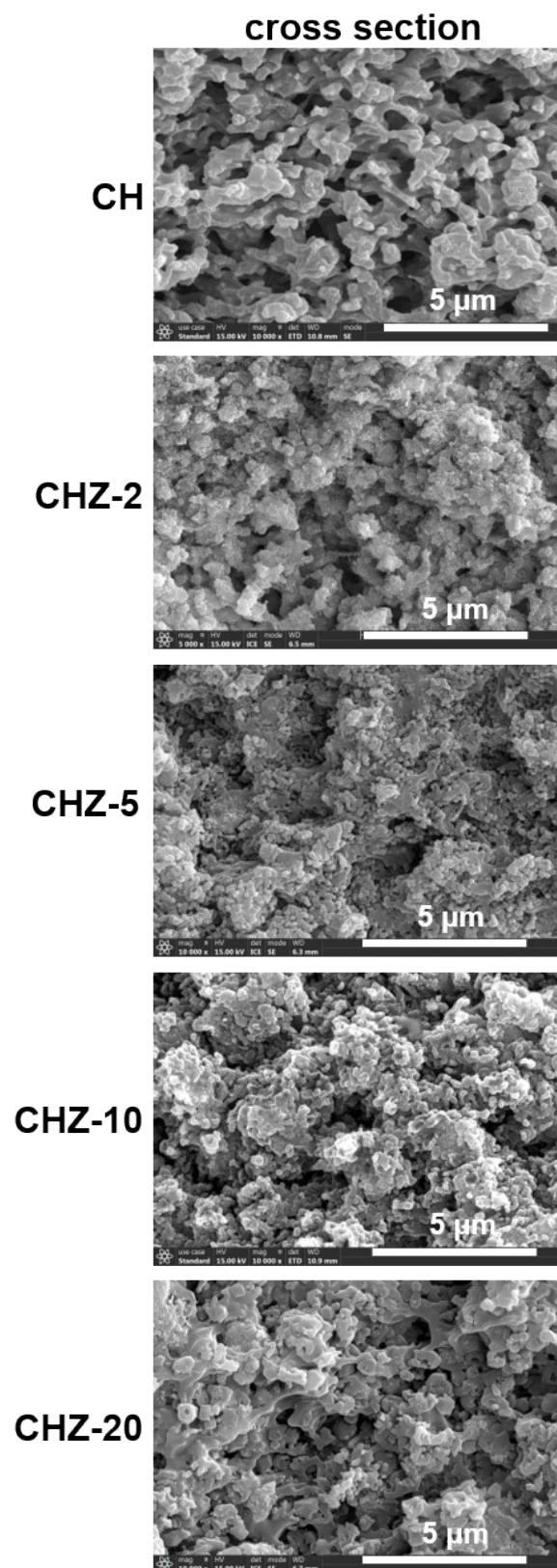


Fig. S4 Cross-section SEM images of CH and CHZ membranes at high magnification. It was clear that as the ZIF-8 load increased, the number of holes in the cross section decreased because of the occupation of the ZIF-8.

Table S2. Porosity of CH and CHZ membranes with different ZIF-8 loading.

Sample number	Porosity of CH (%)	Porosity of CHZ-2 (%)	Porosity of CHZ-5 (%)	Porosity of CHZ-10 (%)	Porosity of CHZ-20 (%)
1 [#]	54.7	49.7	50.4	49.7	36.1
2 [#]	57.1	53.7	52.3	53.7	27.7
3 [#]	59.7	58.7	49.3	58.7	29.4
Average value	57.2 ± 2.5	54.0 ± 4.5	50.7 ± 1.5	45.8 ± 1.3	31.1 ± 4.5

Table S3. Significant difference analysis of swelling ratio about CH, CHZ-2, CHZ-5, CHZ-10, CHZ-20 membranes.

Tukey's multiple comparisons test	Mean Diff.	95.00% CI of diff.	Significant?	Summary	Adjusted P Value
CH vs. CHZ-2	40.13	29.10 to 51.17	Yes	****	<0.0001
CH vs. CHZ-5	46.63	35.60 to 57.67	Yes	****	<0.0001
CH vs. CHZ-10	57.13	46.10 to 68.17	Yes	****	<0.0001
CH vs. CHZ-20	62.6	51.57 to 73.63	Yes	****	<0.0001
CHZ-2 vs. CHZ-5	6.5	-4.532 to 17.53	No	ns	0.3582
CHZ-2 vs. CHZ-10	17	5.968 to 28.03	Yes	**	0.0034
CHZ-2 vs. CHZ-20	22.47	11.43 to 33.50	Yes	***	0.0004
CHZ-5 vs. CHZ-10	10.5	-0.5322 to 21.53	No	ns	0.0639
CHZ-5 vs. CHZ-20	15.97	4.934 to 27.00	Yes	**	0.0053
CHZ-10 vs. CHZ-20	5.467	-5.566 to 16.50	No	ns	0.5121

Table S4. Significant difference analysis of antibacterial activity against *E. coli* about CHZ-2, CHZ-5, CHZ-10, CHZ-20 membranes.

Tukey's multiple comparisons test	Mean Diff.	95.00% CI of diff.	Significant?	Summary	Adjusted P Value
CHZ-2_1 vs. CHZ-2_2	-0.4871	-0.7767 to -0.1974	Yes	***	0.0005
CHZ-5_1 vs. CHZ-5_2	-3.391	-3.680 to -3.101	Yes	****	<0.0001
CHZ-10_1 vs. CHZ-10_2	-4.869	-5.159 to -4.579	Yes	****	<0.0001
CHZ-20_1 vs. CHZ-20_2	-3.897	-4.187 to -3.607	Yes	****	<0.0001
CHZ-2 vs. CHZ-5	-2.49	-2.780 to -2.201	Yes	****	<0.0001
CHZ-5 vs. CHZ-10	-1.346	-1.636 to -1.057	Yes	****	<0.0001
CHZ-10 vs. CHZ-20	0.9754	0.6858 to 1.265	Yes	****	<0.0001

CHZ-2 vs. CHZ-10	-3.837	-4.126 to -3.547	Yes	****	<0.0001
CHZ-5 vs. CHZ-20	-0.3708	-0.6605 to - 0.08116	Yes	**	0.0077
CHZ-2 vs. CHZ-20	-2.861	-3.151 to -2.571	Yes	****	<0.0001

Table S5. Significant difference analysis of antibacterial activity against *S. aureus* about CHZ-2, CHZ-5, CHZ-10, CHZ-20 membranes.

Tukey's multiple comparisons test	Mean Diff.	95.00% CI of diff.	Significant?	Summary	Adjusted P Value
CHZ-2_1 vs. CHZ-2_2	-2.669	-3.194 to -2.145	Yes	****	<0.0001
CHZ-5_1 vs. CHZ-5_2	-6.408	-6.933 to -5.884	Yes	****	<0.0001
CHZ-10_1 vs. CHZ-10_2	-6.75	-7.274 to -6.226	Yes	****	<0.0001
CHZ-20_1 vs. CHZ-20_2	-5.968	-6.492 to -5.443	Yes	****	<0.0001
CHZ-2 vs. CHZ-5	-3.15	-3.674 to -2.626	Yes	****	<0.0001
CHZ-5 vs. CHZ-10	-0.2031	-0.7274 to 0.3212	No	ns	0.8698
CHZ-10 vs. CHZ-20	0.841	0.3167 to 1.365	Yes	***	0.0009
CHZ-2 vs. CHZ-10	-3.353	-3.877 to -2.829	Yes	****	<0.0001
CHZ-5 vs. CHZ-20	0.6379	0.1136 to 1.162	Yes	*	0.0118
CHZ-2 vs. CHZ-20	-2.512	-3.036 to -1.988	Yes	****	<0.0001

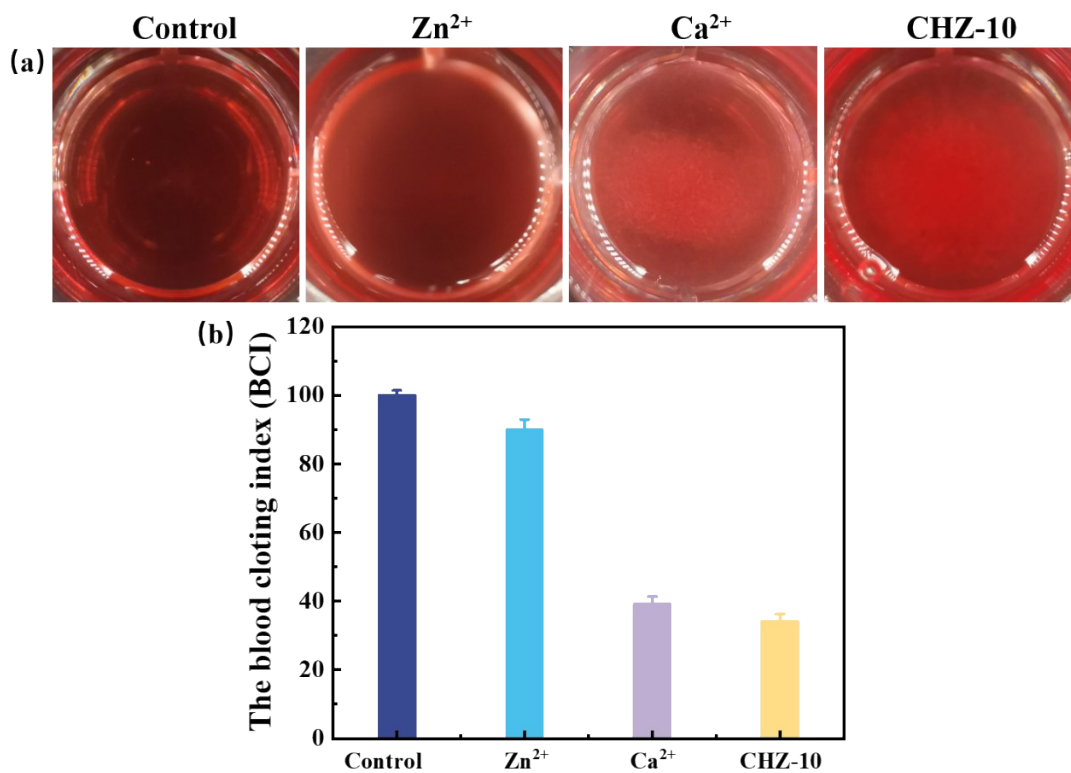


Fig. S5. Images of coagulation effects of control, Zn²⁺, Ca²⁺, and CHZ-10 extracts (a), and the BCI values (b).

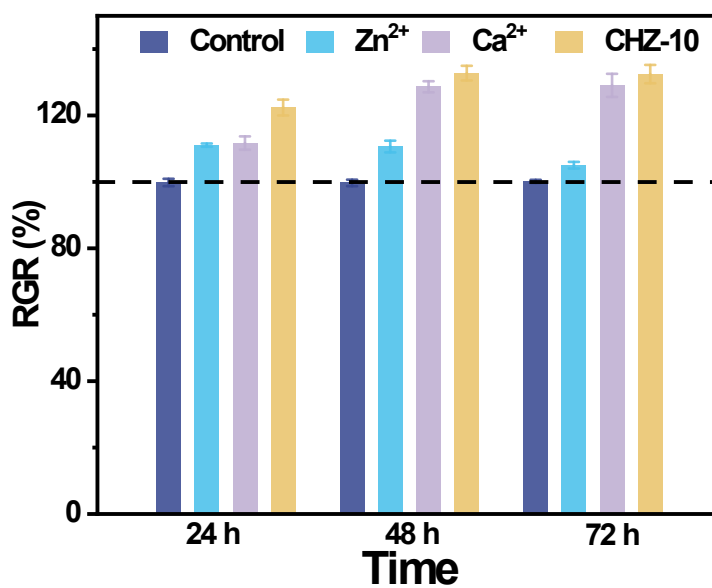


Fig. S6. Cell proliferation of control, Zn²⁺, Ca²⁺ and CHZ-10 extracts at 24, 48 and 72 h.

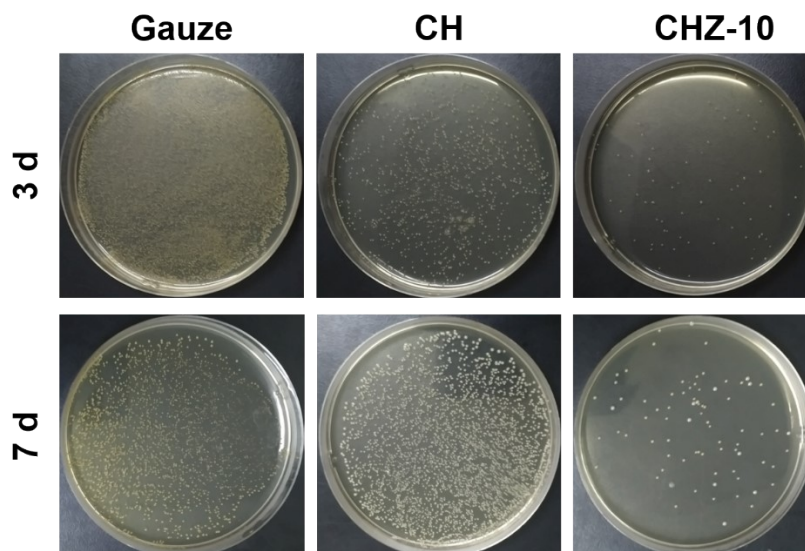


Fig. S7 Bacterial extraction from the infected wounds treated with gauze, CH membrane, and CHZ-10 membrane on days 3 and 7. As shown in Figure S6, the bacteria on the wounds treated with CHZ-10 membrane were significantly lower than those treated with gauze and CH membrane, indicating that CHZ-10 membrane had remarkable antibacterial activity *in vivo*.

Table S6. Comparison of CHZ-10 with other chitosan and ZIF-8 composite antimicrobial materials.

Materials	Structural morphology	Antibacterial type	Evaluation methods	Antibacterial efficiency	Mechanism	<i>In vivo</i> animal experimental models	Ref.
Chitosan/Pseudo-Protein Hybrid Hydrogels	three-dimensional microporous	<i>E. Coli</i> <i>S. aureus</i>	viable cell counting	91.81% 85.59%	activated both NO and TNF- α	no	5
Carboxymethyl chitosan/polyurethane-gelatin hydrolysate	-	<i>E. Coli</i> <i>S. aureus</i>	zone of inhibition	20 mm 16 mm	-	no	6
Ag-Phy@ZIF-8@HA	core-shell nanoparticles	<i>E. Coli</i> <i>S. aureus</i>	viable cell counting	99.1% 99.5%	pH-responsive release of $^{70}\text{Zn}^{2+}$ and Ag^+	no	8
Cu(II)@ZIF-8 nanoparticles	nanoparticles	<i>E. Coli</i> <i>S. aureus</i>	viable cell counting	-	dual enzyme-like activity	no	9
ZIF-8@Levo/LBL	-	<i>E. Coli</i> <i>S. aureus</i>	viable cell counting	-	pH-responsive release of Zn^{2+} and Levo	a rat model with <i>S. aureus</i> -infection	10

Cu-doped ZIF-8	nanoparticles	<i>E. Coli</i> <i>S. aureus</i>	viable cell counting	99.37% 99.98%	initiative ROS generation	no	11
Copper@ZIF-8	core-shell nanowires	<i>E. Coli</i> <i>S. mutans</i>	measuring optical density	91% 86%	release of Cu ²⁺	no	7
Bacterial cellulose@ε-polylysine Membrane	porous structure	<i>E. Coli</i> <i>S. mutans</i>	viable cell counting	99.83% 96.9%	-	a rat model with <i>S. aureus</i> -infection	12
HCZ-10	porous structure	<i>E. Coli</i> <i>S. mutans</i>	zone of inhibition	13.3 mm 11.5 mm	pH-responsive release of Zn ²⁺	a rat model with <i>S. aureus</i> -infection	This work

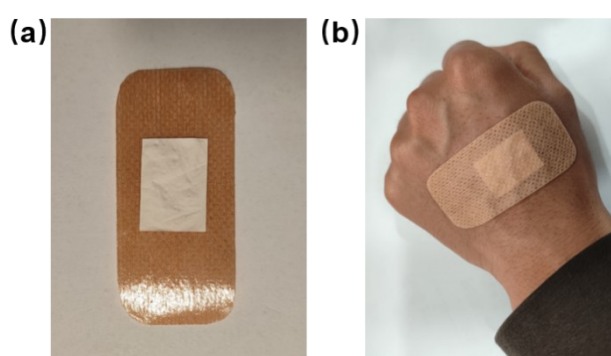


Fig. S8 Preparation of CHZ-10 as a portable wound dressing. Photograph of the appearance of the portable wound dressing (a); photograph of the portable wound dressing acting on real skin surfaces.

References

1. H. Fang, J. Wang, L. Li, L. Xu, Y. Wu, Y. Wang, X. Fei, J. Tian and Y. Li, *Chemical Engineering Journal*, 2019, **365**, 153-164.
2. H. Chen, J. Zhang, H. Wu, Y. Li, X. Li, J. Zhang, L. Huang, S. Deng, S. Tan and X. Cai, *ACS Applied Bio Materials*, 2021, **4**, 6137-6147.
3. M. He, F. Ou, Y. Wu, X. Sun, X. Chen, H. Li, D. Sun and L. Zhang, *Materials & Design*, 2020, **194**, 108913.
4. X. Yuehua, F. Yan, O. Yanjing, Y. Liyu, C. Qinhuai, S. Caixia, C. Jiang and L. Haiqing, *ACS Sustainable Chemistry & Engineering*, 2020, **8**, 18915–18925.
5. M. Yin, S. Wan, X. Ren and C.-C. Chu, *ACS Applied Materials & Interfaces*, 2021, **13**, 14688-14699.
6. M. Zhang, M. Yang, M. W. Woo, Y. Li, W. Han and X. Dang, *Carbohydrate Polymers*,

- 2021, **256**, 117590.
7. A. Kumar, A. Sharma, Y. Chen, M. M. Jones, S. T. Vanyo, C. Li, M. B. Visser, S. D. Mahajan, R. K. Sharma and M. T. Swihart, *Advanced Functional Materials*, 2021, **31**, 2008054.
 8. L. Tan, G. Yuan, P. Wang, S. Feng, Y. Tong and C. Wang, *International Journal of Biological Macromolecules*, 2022, **206**, 605-613.
 9. C. Zhang, Z. Shu, H. Sun, L. Yan, C. Peng, Z. Dai, L. Yang, L. Fan and Y. Chu, *Applied Surface Science*, 2023, **611**, 155599.
 10. B. Tao, W. Zhao, C. Lin, Z. Yuan, Y. He, L. Lu, M. Chen, Y. Ding, Y. Yang, Z. Xia and K. Cai, *Chemical Engineering Journal*, 2020, **390**, 124621.
 11. X. Wang, H. Wang, J. Cheng, H. Li, X. Wu, D. Zhang, X. Shi, J. Zhang, N. Han and Y. Chen, *Chemical Engineering Journal*, 2023, **466**, 143201.
 12. F. Wahid, X.-J. Zhao, X.-Q. Zhao, X.-F. Ma, N. Xue, X.-Z. Liu, F.-P. Wang, S.-R. Jia and C. Zhong, *ACS Applied Materials & Interfaces*, 2021, **13**, 32716-32728.